

Implementing robust amyloid PET quantification in multi-center studies: AMYPAD approach to address data acquisition, processing, interpretation and data sharing challenges

Ariane Bollack^{1,2}  | Mahnaz Shekari^{3,4,5}  | Lyduine E. Collij^{6,7,8}  |
 Emma Luckett⁶  | David Valléz García^{3,6}  | Paweł Markiewicz^{2,9,10}  |
 Robin Wolz¹¹ | Maqsood Yaqub⁶  | Alle Meije Wink⁶ | Rossella Gismondi¹² |
 Andrew Stephens¹² | Pieter Jelle Visser⁶  | Anja Mett¹ |
 Alexander Drzezga^{13,14,15}  | Christopher Buckley¹  | Juan Domingo Gispert^{3,4,5}  |
 Gill Farrar¹  | Frederik Barkhof^{2,6,7,16} 

¹GE HealthCare, London, UK

²Department of Medical Physics and Biomedical Engineering, University College London, London, UK

³Barcelonaβeta Brain Research Center, Pasqual Maragall Foundation, Barcelona, Spain

⁴Hospital del Mar Medical Research Institute (IMIM), Barcelona, Spain

⁵Universitat Pompeu Fabra, Barcelona, Spain

⁶Department of Radiology & Nuclear Medicine, Amsterdam UMC, Vrije Universiteit, Amsterdam, The Netherlands

⁷Brain Imaging, Amsterdam Neuroscience, Amsterdam, The Netherlands

⁸Clinical Memory Research Unit, Department of Clinical Sciences Malmö, Faculty of Medicine, Lund University, Malmö, Sweden

⁹School of Computer Science and Digital Technology, LSBU, Southwark, UK

¹⁰Royal Free London NHS Foundation Trust, London, UK

¹¹IXICO, London, UK

¹²Life Molecular Imaging GmbH, Berlin, Germany

¹³Department of Nuclear Medicine, University Hospital Cologne, Köln, Germany

¹⁴German Center for Neurodegenerative Diseases (DZNE), Bonn, Germany

¹⁵Institute of Neuroscience and Medicine–Molecular Organization of the Brain (INM-2), Forschungszentrum Jülich, Jülich, Germany

¹⁶Queen Square Institute of Neurology, University College London, London, UK

Correspondence

Ariane Bollack, GE HealthCare, Pollard Woods,
Nightingales Lane, Chalfont St Giles,
Buckinghamshire, HP8 4SP, UK.

Email: ariane.bollack@gehealthcare.com

Abstract

INTRODUCTION: Amyloid-positron emission tomography (PET) is pivotal to Alzheimer's management, with the Centiloid standardizing measurements across tracers. AMYPAD trials (Diagnostic and Patient Management Study [DPMS] and

Funding information

Innovative Medicines Initiative, Grant/Award Number: 115952; Alzheimer's Disease Data Initiative

Prognostic and Natural History Study [PNHS]) aimed to validate robust quantification in clinical settings. We report our comprehensive approach to amyloid-PET implementation, comprising scan acquisition, harmonization, data storing, and data sharing strategies.

METHODS: Data from 28 scanners were harmonized using Hoffman phantoms. Three quantification workflows were compared: AmyPype (PET-only), IXICO-LEAP, and the standard Centiloid pipeline (magnetic resonance imaging [MRI]-based). Distributions of Centiloids were assessed using Gaussian Mixture Modeling.

RESULTS: Binary quantification showed excellent concordance between pipelines ($\geq 96\%$) and compared to visual reads ($>90\%$). DPMS Centiloids had a bimodal distribution while the PNHS showed a more skewed distribution toward higher Centiloids modeled with three Gaussians ($1^{\text{st}} \text{ Gaussian mean} + 2\text{SD} = 12 \text{ CL, emerging pathology}$).

DISCUSSION: The harmonization framework, providing strong cross-method correlations in AMYPAD, has been adopted by EARL as the Brain PET/CT accreditation standard and provides a practical approach for other multi-center cohorts to implement similar strategies.

KEYWORDS

Alzheimer's, amyloid, Centiloid, PET, quantification

Highlights

- We share AMYPAD's end-to-end approach to amyloid positron emission tomography (PET) quantification from data acquisition and handling, harmonization based on Hoffman phantoms, quality control, image processing, to data storage, and data sharing strategies.
- Centiloid quantification was compared across one PET-only (AmyPype) and two PET-MR pipelines (standard Centiloid and IXICO-LEAP). Excellent agreement in dichotomized Centiloid values was observed both between pipelines and when compared to visual reads.
- Distribution of Centiloid values in the Prognostic and Natural History Study (PNHS) and Diagnostic and Patient Management Study (DPMS) are in line with the initial recruitment strategies of the trials.
- Harmonization of Amyloid-PET scans framework was adopted by EARL as the Brain PET/CT accreditation standard for multicentre brain PET scans.

1 | INTRODUCTION

Amyloid-beta ($A\beta$) positron emission tomography (PET) detects the presence and spread of amyloid plaques in the brain, one of the earliest pathological hallmarks of Alzheimer's disease (AD).¹ Three Fluorine-18 amyloid-PET tracers have been regulatory-approved for routine clinical use: [¹⁸F]florbetapir (Amyvid™; Eli Lilly),² [¹⁸F]flutemetamol (Vizamyl™; GE HealthCare),³ and [¹⁸F]florbetaben (Neuraceq®; Life Molecular Imaging).⁴ Amyloid-PET has shown clinical value in terms of increased diagnostic confidence and changes in patient management.⁵

and is widely used to study the natural history of AD and in disease modifying therapies trials.^{6,7}

In clinical settings, amyloid-PET is usually assessed visually by a trained specialist and rated as negative or positive. Recently, three major developments have led to the use of quantification as adjunct to visual read. First, AD diagnosis is more often made in an early stage of the disease, where emerging $A\beta$ pathology challenges high confidence assessments.⁸ Second, this shift toward earlier diagnoses has led to improvements in risk stratification of pre-dementia patients.^{9,10} Thirdly, anti-amyloid therapies requires the accurate identification of

$\text{A}\beta$ pathology and assessment of treatment effects. Quantification provides a continuous measure of amyloid burden, and is likely to become essential in managing patients receiving amyloid-removing therapies. Therefore, establishing accurate and robust methods for amyloid-PET quantification is paramount.

Quantification of amyloid-PET has traditionally been performed using the standardized uptake value ratio (SUVR) at a tracer equilibrium time interval. However, several shortcomings including between-tracer differences limit the utility of this metric.¹¹ To overcome those, the Centiloid approach was proposed providing a standardized scale of amyloid load irrespective of the amyloid tracer and processing pipeline.¹² This scale is based on converting ¹⁸F-amyloid tracers SUVR to the ¹¹C-PiB-equivalent SUVR and anchoring the values between 0 (mean level of amyloid PET tracer uptake in young controls) and 100 (average signal observed in typical mild-to-moderate AD dementia patients). It is now widely implemented in current clinical trial design and can become a practical and valuable metric for routine clinical use of quantitative PET.^{11,13} Indeed in 2024, the European Medicines Agency endorsed a Biomarker Qualification Opinion on the Centiloid scale (EMADOC-1700519818-1200791).

In order to optimize the use of amyloid-PET, the amyloid imaging to prevent Alzheimer's disease (AMYPAD) consortium was set up in 2016. AMYPAD is a collaborative research program with the aim to improve understanding, diagnosis, and management of AD through the utilization of amyloid-PET. The project consisted of two trials: (1) Diagnostic and Patient Management Study (DPMS)¹⁴ focused on patients with AD across the disease continuum and the (2) Prognostic and Natural History Study (PNHS)¹⁵ focused on a population without a dementia diagnosis.

By leveraging data collected within AMYPAD, the consortium aimed to determine the applicability of quantification for both research and clinical settings. This was supported by the validation of the Centiloid metric and the implementation of consistent and reproducible image interpretation across multi-center studies. Another priority for the consortium was to enable the integration of additional datasets and facilitate collaborative access to the collected data.

In this work, we present the amyloid-PET standards for quantification implemented across the two AMYPAD trials, relying on extensive amyloid-PET harmonization efforts across 17 sites and cross-validation of three Centiloid pipelines, providing a practical approach for other multi-center cohorts to implement similar strategies.

2 | MATERIALS AND METHODS

2.1 | Description of AMYPAD cohorts: DPMS and PNHS

2.1.1 | DPMS

The DPMS involved eight centers and completed its enrolment of 844 memory clinic patients suspected of AD in June 2020.¹⁶ In the DPMS, $\text{A}\beta$ burden was primarily assessed by visual reading, as per standard

RESEARCH IN CONTEXT

1. **Systematic review:** The authors reviewed the literature using traditional sources, meeting abstracts and presentations (PubMed, Google Scholar). Amyloid positron emission tomography (PET) quantification workflows in multi-centre cohorts often primarily and sometimes solely focus on data processing.
2. **Interpretation:** We propose an end-to-end approach covering data acquisition and handling, harmonization based on Hoffman phantoms, quality control, image processing, to data storage, and data sharing strategies. These were effective to ensure consistent amyloid PET interpretation across multi-center European studies. Distribution of Centiloid values in the Prognostic and Natural History Study (PNHS) and Diagnostic and Patient Management Study (DPMS) are in line with the initial recruitment strategies of the trials.
3. **Future directions:** Amyloid-PET data from AMYPAD is now available for all researchers on ADDI. The DPMS and PNHS datasets are well-positioned to help refine the role of amyloid-PET for optimal diagnostic and management of Alzheimer's, as well as to study the natural progression of the disease, and get deeper insights into factors of resilience.

clinical routine at the time. Quantification of $\text{A}\beta$ burden was performed for secondary analyses. Other imaging modalities, including structural magnetic resonance imaging (MRI), were acquired according to local practice, and not systematically available for quantitative purposes. As a result, this dataset required a PET-only quantification pipeline.

2.1.2 | PNHS

The PNHS involved 17 sites and completed the enrolment of >1600 participants in June 2022.¹⁵ The PNHS was a natural history study that aimed to evaluate how $\text{A}\beta$ imaging could improve understanding the natural course of AD and modeling biomarker trajectories along preclinical stages. The study used amyloid-PET imaging as an additional and relevant AD biomarker to complement the phenotypical characterization of participants in 11 European parent study cohorts, including the European Prevention of Alzheimer's Dementia Longitudinal Cohort Study (EPAD LCS),¹⁷ European Medical Information Framework for Alzheimer's Disease (EMIF-AD) 60+¹⁸ and 90+, Alzheimer's and Family + (ALFA+),¹⁹ FundacioACE Healthy Brain Initiative (FACEHBI),²⁰ (Flemish Prevent Alzheimer's Disease Cohort KU Leuven) F-PACK,²¹ UCL-2010-412, Microbiota, AMYPAD DPMS (via the Amsterdam University Medical Center [AUMC]),¹⁶ DZNE-Longitudinal Cognitive Impairment and Dementia

Study (DELCODE),²² and Gothenburg H70 Birth cohort study^{23,24}. Accurate quantitative measurements of A β burden were central to the project objectives. Therefore, research-quality 3D-T1 weighted MRI scans were acquired to aid the analysis of amyloid-PET scans with a substantial subset of participants underwent dual-time window acquisition protocols.²⁵

2.2 | Amyloid-PET acquisition protocols

Complete explanations of the procedures below are available in Supporting Information—Appendix A.

2.2.1 | Site setup, image management, and image quality control

IXICO oversaw scanner qualifications and data collection for both studies, ensuring compliance with European Union (EU) data protection regulations via its Trial Tracker platform. Images stored included PET (attenuation-corrected and uncorrected) in DICOM format, and any computed tomography (CT) or MRI images.

Prior to participant scanning, each site underwent qualification using a phantom to assess adherence to specific imaging protocol, image quality control, and appropriate quantitative performance as per European Association of Nuclear Medicine Research Ltd. (EARL) guidelines.²⁶ For the DPMS study, suitable images were transferred to GE HealthCare for technical and scientific quality checks, followed by amyloid quantification using AmyPype,²⁷ with dynamic data sent to AUMC for parametric analysis (see imaging workflow in Figure 1A). For PNHS, images underwent rigorous quality inspection, including brain coverage, head positioning, signal-to-noise ratio, and motion artifacts, before analysis via IXICO's pipeline; dual-phase images were sent to AUMC for dynamic analysis, with further quality control checks on metadata and motion alignment. The imaging workflow is imaged in Figure 1B.

2.2.2 | Static acquisition protocol: DPMS and PNHS

As per the product label, scans were acquired according to the static imaging protocol. This entailed acquisition at 90 min post-injection (p.i.) of 300 MBq ($\pm 20\%$) [^{18}F]florbetaben/Neuraceq® (FBB) and 185 MBq ($\pm 10\%$) [^{18}F]flutemetamol/Vizamyl (FMM) and collected in four frames of 5 min each.^{28,29}

The dynamic (dual-time window) acquisition protocol can be found in the Supporting Information—Appendix B.

2.2.3 | Harmonization of amyloid PET scans

Amyloid brain PET scans in the DPMS and PNHS studies were acquired from 28 different scanners using site-specific reconstruction param-

eters, introducing significant heterogeneity in image properties and potential bias in cerebral A β load estimation. To address this, a new harmonization protocol was developed in collaboration with EARL within the AMYPAD study,³⁰ and is now adopted as the Brain PET/CT accreditation standard. This method involved acquiring 3D Hoffman phantom scans at each site with their specific reconstruction protocol, calculating the effective image resolution of the reconstructions, and applying Gaussian post-smoothing filters to match the lowest resolution across sites (Figure 2). This approach ensured consistent and reliable global and regional quantitative metrics for pooled data, and reduced post-processing errors. While MRI protocol variability across parent cohorts posed an additional challenge, robust brain segmentation methods minimized its impact, keeping SUVR variability within scan-rescan variability, and significantly lower than the variability observed in amyloid-rich regions of interests (ROIs). This finding suggests that even when MR protocol differ, its impact on the PET analysis is mitigated by the actual difference in PET resolution.

2.3 | Visual assessment of amyloid-PET images

Visual interpretation of PET images was performed using a standardized and blinded method by trained nuclear physicians or radiologists who had followed the tracer-specific reader training. Details on read methodologies and reporting can be found in Supporting Information—Appendix C.

2.4 | Static PET quantification

2.4.1 | DPMS: PET-only pipeline | AmyPype software

For the DPMS, AmyPype was designed to allow the harmonized quantitative assessment of [^{18}F]flutemetamol and [^{18}F]florbetaben amyloid-PET without the need for an individual's structural MRI images.^{27,31}

In AmyPype, late-phase PET-only images undergo frame-to-frame alignment. Summed images are spatially normalized to the standard Montreal Neurological Institute (MNI152) space using an adaptive template registration method.³² Briefly, this method uses an adaptive template consisting of two tracer-specific images in the standard space, whose linear combination can generate the optimal template for registering any given amyloid-PET scan. Next, the Centiloid Cortical target mask is applied to the images, as well as a gray-matter parcellated cortical-volume of interest mask, consisting of the regions in the Automated Anatomical Labeling atlas³³ that typically accumulate A β . The whole cerebellum is used as reference region (Figure 3). The volume of interest overlayed on the PET image data is checked visually from AmyPype quality control output. In case of any observations/issues, these were recorded in the quantitation report and when necessary, sites were provided feedback.

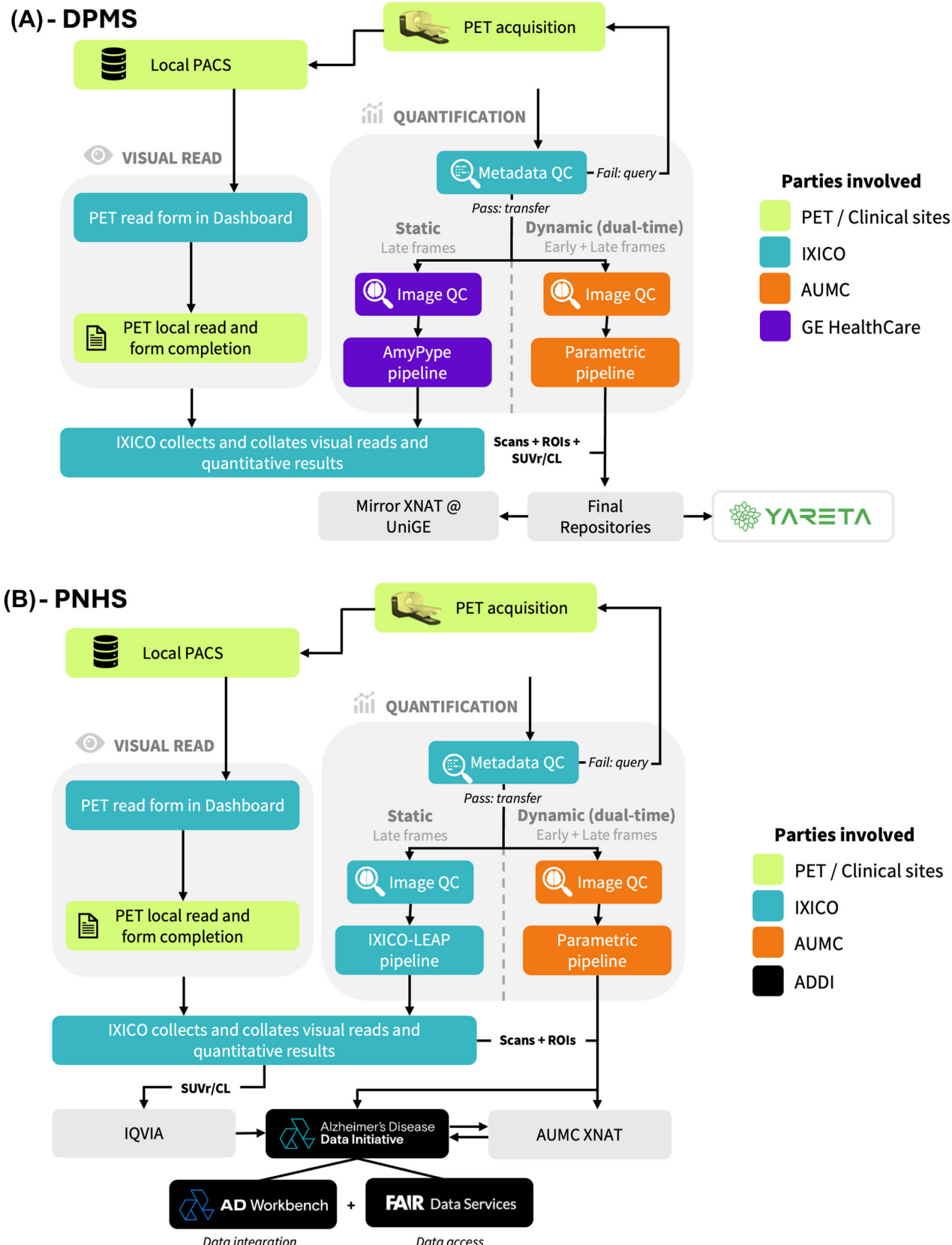


FIGURE 1 Imaging data flow in the DPMS (A) and PNHS (B). The parametric pipeline corresponds to the dynamic data processing workflow, which is described in the [Supporting Information](#). DPMS, Diagnostic and Patient Management Study; LEAP, learning embeddings for atlas propagation; PACS, picture archiving and communication system; PNHS, Prognostic and Natural History Study; QC, quality control.

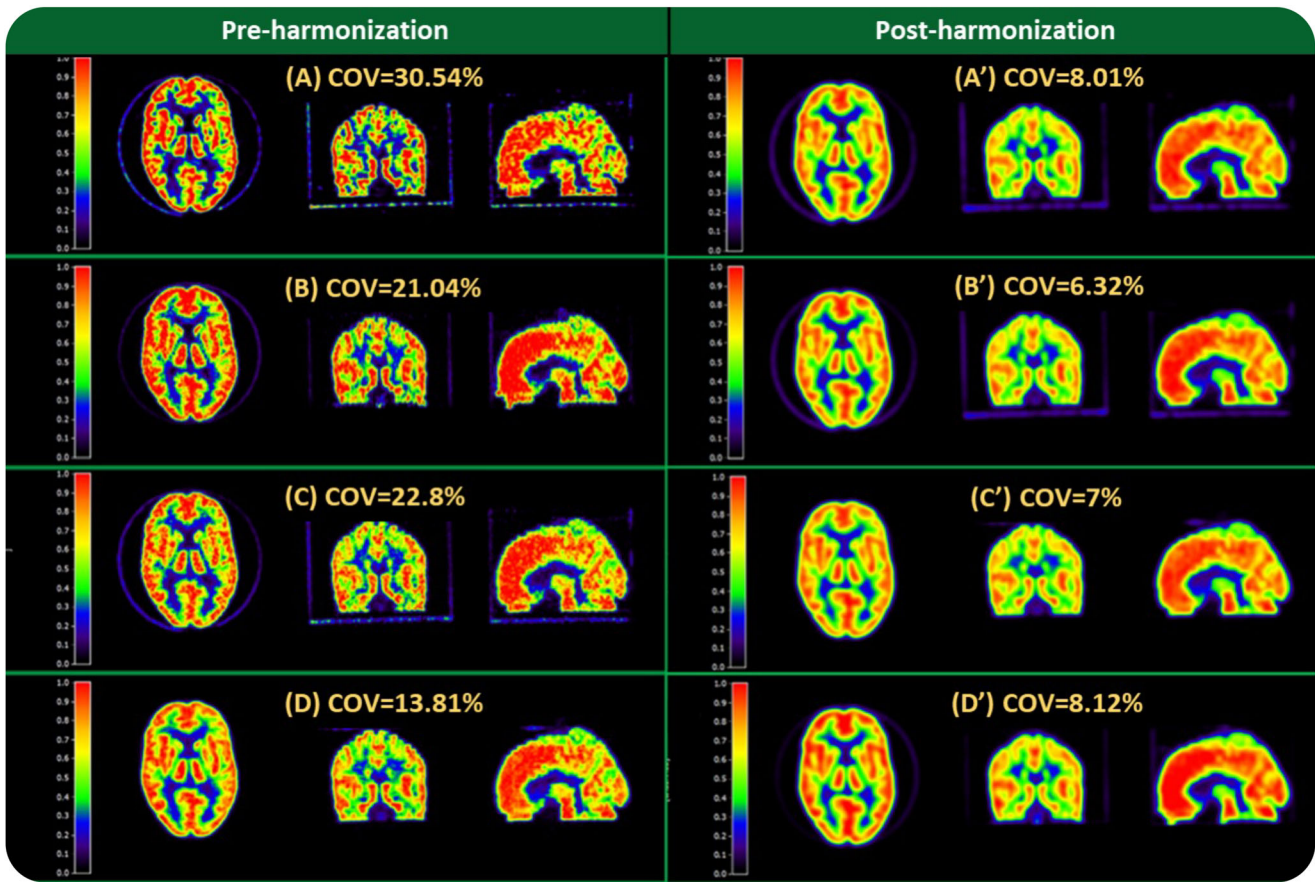


FIGURE 2 Examples of Hoffman phantom scans from four AMYPAD imaging sites, shown before (left) and after (right) harmonization.²⁹ Units in the colorscale represent voxel intensity normalized to the activity concentration. After harmonization, the coefficient of variance (COV%)—an indicator of image heterogeneity—shows comparable values across all sites. The COV% corresponds to the ratio of the standard deviation of the activity concentration in five regions of interest drawn on the white matter, over the mean activity concentration in these regions (x100).

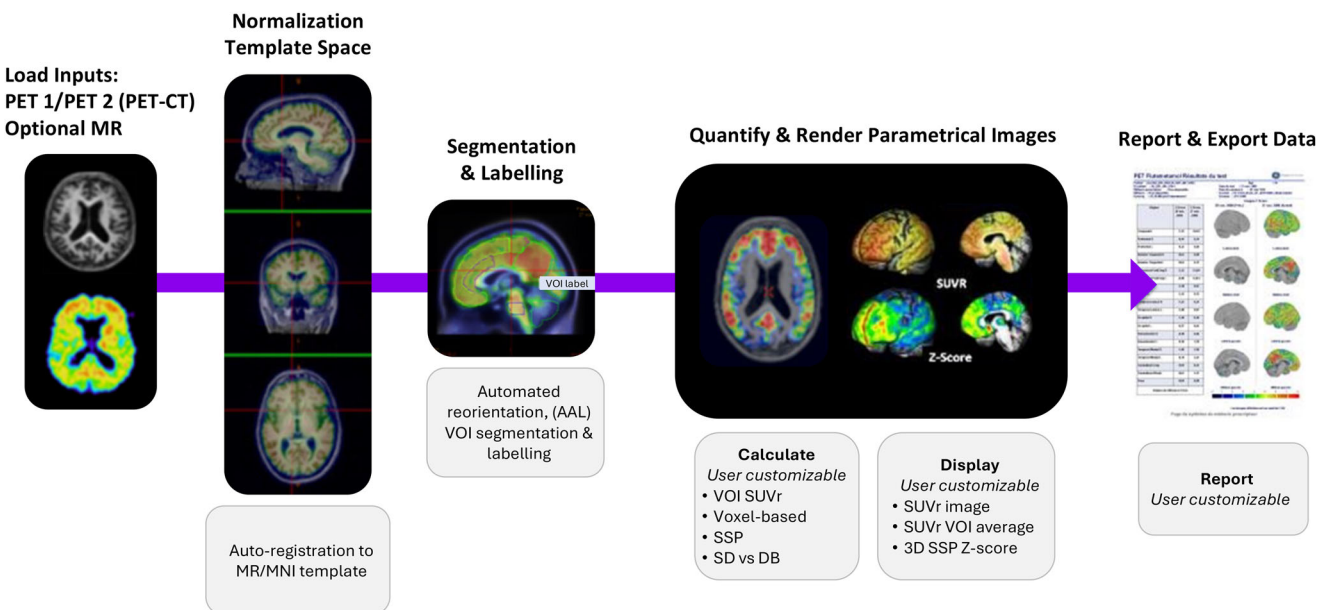


FIGURE 3 AmyPipe: PET-only pipeline built on CortexID Suite for the analysis of the DPMS scans. It is based on the adaptive-normalization of $\text{A}\beta$ PET scans, and outputs SUVR, Z-scores, and Centiloid values for both $[^{18}\text{F}]\text{flutemetamol}$ and $[^{18}\text{F}]\text{florbetaben}$ scans. $\text{A}\beta$, amyloid-beta; DPMS, Diagnostic and Patient Management Study; PET, positron emission tomography; SUVR, standardized uptake value ratio.

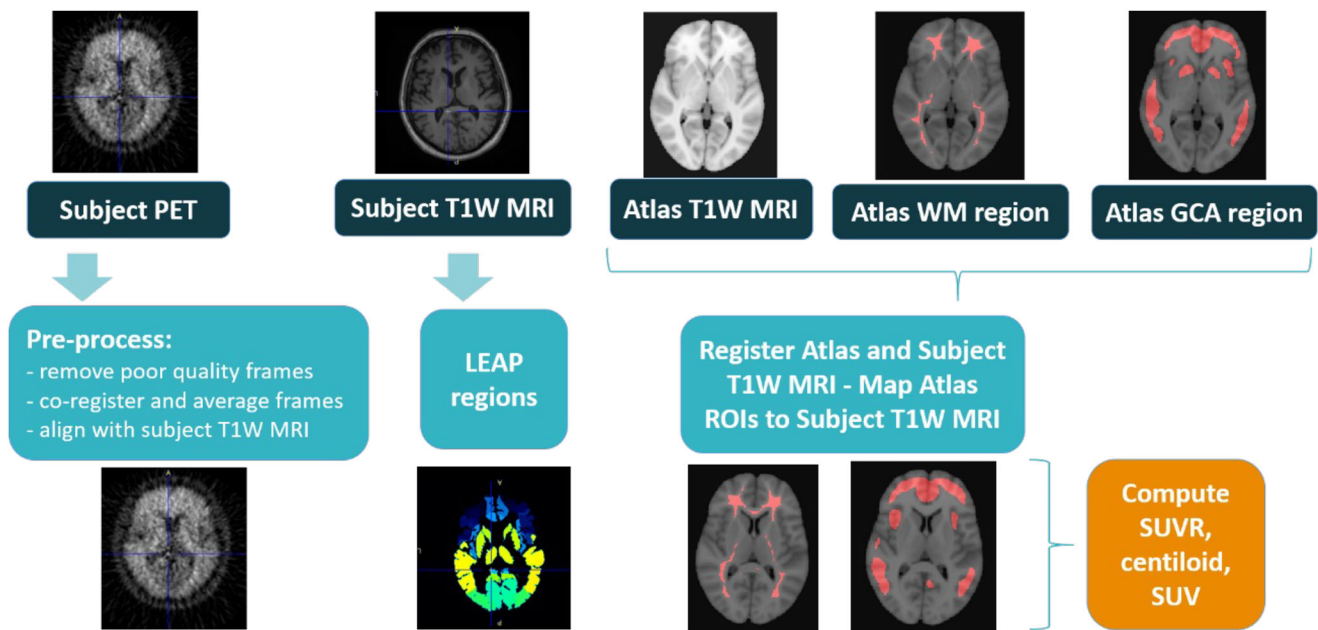


FIGURE 4 IXICO-LEAP workflow: MR-based quantification pipeline built on LEAP for the PNHS. This method works in the subject's space by co-registering PET scans with their corresponding MR scan, which was parcellated using the LEAP method. Two target regions were used: the GAAIN global cortical average and a composite of cortical LEAP regions (see *Supporting Information*–Appendix D for the list of regions). Reference regions were all based on the LEAP parcellation. This pipeline was calibrated to render comparable Centiloid values for both $[^{18}\text{F}]\text{flutemetamol}$ and $[^{18}\text{F}]\text{florbetaben}$ scans, on top of SUV and SUVR values. GAAIN, Global Alzheimer's Association Interactive Network; LEAP, learning embeddings for atlas propagation; MR, magnetic resonance; PET, positron emission tomography; PNHS, Prognostic and Natural History Study; SUV, standardized uptake value; SUVR, standardized uptake value ratio.

Users can request access to AmyPype through the following contact: amypype.downloads@gehealthcare.com.

2.4.2 | PNHS: PET and MR pipeline | IXICO in-house workflow "IXICO-LEAP"

For all scans marked suitable for analysis in the PNHS study, SUVR, and Centiloid computation were performed using IXICO's in-house fully automated regional SUVR workflow.

To maximize the quantitative accuracy of individual $\text{A}\beta$ load, this method employed a subject-specific multi-atlas structural MRI segmentation approach named learning embeddings for atlas propagation (LEAP;^{34,35}), which allows for flexibly selecting multiple single and/or composite regions for the analysis. In this article, the workflow is referred to as "IXICO-LEAP".

IXICO-LEAP methodology consisted of co-registering PET frames and creating an average image aligned to the corresponding MRI scan. The MRI scan was then parcellated using the multi-atlas LEAP methodology, and these masks were used to compute SUVR and Centiloid values in native space (Figure 4). Apart from computing SUVR for regions defined in IXICO's LEAP atlas (full list in *Supporting Information*–Appendix D), standard space templates were incorporated to include additional regions. In this case, standard space templates were used to define the Global Alzheimer's Association Interactive Network (GAAIN) global cortical average region in

the native space, and the Harvard–Oxford white matter reference region,³⁶ which was then additionally refined using morphological operations to ensure that non-white-matter tissue was excluded. The analysis was then implemented in a validated and centralized computer system and overseen by IXICO's in-house trained image analysts.

Dynamic quantification is described in *Supporting Information*–Appendix B.

2.5 | Statistical analysis

In total, 51 scans from the DPMS were processed with AmyPype, the IXICO-LEAP workflow, and the standard Centiloid pipeline, and all scans from the PNHS were processed with the latter two, allowing head-to-head comparison with correlation and Bland–Altman plots. For each pair of pipelines, performance metrics used were the correlation coefficient R^2 , intercept, slope, and 95% limits of agreement (mean difference ± 1.96 standard deviation [SD]). Agreement with visual read was also considered based on the percentage of concordant/discordant cases and Cohen's kappa. In these scenarios, CL values were dichotomized using a 24.4 CL cutoff, chosen from an independent histopathology-based threshold (detecting moderate-to-frequent neuritic plaques based on the Consortium to Establish a Registry for Alzheimer's Disease [CERAD] score³⁷). We also included percentage agreement between pipeline and kappa scores around the three

clinically-relevant thresholds from the donanemab phase III trial (11, 25, and 37 CL),⁶ in Supporting Information–Appendix E.

In addition, quantification results are shown across clinical groups, compared between radiotracers (i.e., FBB and FMM), and against visual read status (i.e., negative/positive). In the DPMS, clinical groups correspond to individuals with subjective cognitive decline +, mild cognitive impairment or dementia. In the PNHS, clinical groups were defined as cognitively unimpaired (CU) and cognitively impaired (CI) based on a Clinical Dementia Rating scale (CDR) of 0 or 0.5 respectively. A Gaussian Mixture Modeling (GMM) was performed on the distribution of CL values in the DPMS and the PNHS, using the Akaike Information Criterion (AIC) to select the number of Gaussian functions that best model the data.

All statistical analyses were performed in R version 4.3.1.

2.6 | Data sharing

The PNHS dataset, containing the tabulated harmonized clinical and biomarker data, is available for individuals via a formal data access request on the Alzheimer's Disease Data Initiative Work-Bench (ADWB) and their Findability, Accessibility, Interoperability, and Reusability (FAIR) Data Service.³⁸ Users can create an account and a dedicated Workspace on the ADWB in which they host the data and perform their analyses. Furthermore, preprocessed PET scans are available via the Health RI XNAT platform,³⁹ the request for which is also made via the ADWB and FAIR Data Service.

3 | RESULTS

3.1 | Comparison of Centiloid quantification pipelines

Three Centiloid pipelines were compared: AmyPype, IXICO-LEAP workflow, and the standard Centiloid pipeline, using data from the DPMS and PNHS.

Global demographic characteristics were described in details previously for the two cohorts.^{15,16} In the subset of 51 scans from the DPMS processed with all three pipelines, the mean age was 70.2 ± 7 years old, 27% of participants were female, 53% had a CDR of 0.5, and 47% were visually positive (split between tracers: FBB, $N = 44$; FMM, $N = 7$).

IXICO-LEAP pipeline and the standard Centiloid pipeline were strongly correlated with minimal bias, both in the PNHS and in the subset of the DPMS data processed with those workflows (Figure 5A,B: $R^2 > 0.96$, slope from 0.94 to 0.97, intercept from 1.4 to 3.3 CL, limits of agreement $\sim[-13, 9]$ CL). In the sub-sample of 51 scans from the PNHS processed with all three pipelines, the AmyPype software was also highly correlated with the standard Centiloid pipeline, with a negative shift in the intercept and notable variability at the individual level (Figure 5B: $R^2 = 0.96$, slope = 1, intercept = -6.7 CL, limits of agreement $\sim[-21, 12]$ CL). Similar trends were observed when compared to

the IXICO-LEAP pipeline ($R^2 = 0.94$, slope = 1.1, intercept = -7.3 CL, limits of agreement $\sim[-26, 19]$ CL).

Next, focusing on dichotomized of CL values around 24.4 CL as positivity threshold, the percentage agreement between pipelines was very high in both in the DPMS and in the PNHS (Figure 5C: Concordant binary assessment in the DPMS: $49/51 = 96\%$ and in the PNHS: $1495/1542 = 97\%$). In the PNHS, the amyloid load of the 47 scans with discordant results ($\text{Pos}_{\text{Standard}}/\text{Neg}_{\text{IXICO-LEAP}}: N = 10$; $\text{Pos}_{\text{IXICO-LEAP}}/\text{Neg}_{\text{Standard}}: N = 37$) were in the intermediate 10–30 CL range (Standard pipeline: 22 ± 5 CL; IXICO-LEAP: 26 ± 4 CL).

Last, the percentage agreement between CL quantification and visual reads was high for all three software, both in the DPMS and PNHS datasets (Figure 5D: concordance cases $>90\%$). Cohen's kappa were also high in the PNHS ($\kappa_{\text{Standard}} = 0.79$ [0.77, 0.82]; $\kappa_{\text{IXICO-LEAP}} = 0.8$ [0.74, 0.8]) and in the DPMS ($\kappa_{\text{Standard}} = 0.85$ [0.72, 0.98]; $\kappa_{\text{IXICO-LEAP}} = 0.9$ [0.76, 0.99]; $\kappa_{\text{AmyPype}} = 0.8$ [0.67, 0.96]). Focusing on the 10–60 CL range in the PNHS data ($N = 465$), the agreement between quantification and visual read was lower (standard pipeline: 79.8% concordance, $\kappa_{\text{Standard}} = 0.56$ [0.48, 0.64]; IXICO-LEAP: 75.6% concordance, $\kappa_{\text{IXICO-LEAP}} = 0.5$ [0.41, 0.57]). The majority of the discordant cases were Centiloid positive (>25)/visual read negative (standard pipeline: 13.5% $\text{CL}_{\text{Standard}} + / \text{VR} -$; IXICO-LEAP: 18.6% $\text{CL}_{\text{IXICO-LEAP}} + / \text{VR} -$). Details of agreement with visual reads across tracers and levels of read confidence can be found in Supporting Information–Appendix E.

Subsequent analysis results were obtained using the Standard CL pipeline for the PNHS and the AmyPype pipeline for the DPMS.

3.2 | Distribution of Centiloids in the DPMS and PNHS

Figure 6A shows the frequency distribution of the Centiloid values for 729 baseline scans of the DPMS. The data presents a bimodal distribution as expected from the sampling of clinical populations. For the DPMS, the optimal number of Gaussians was two, corresponding to the “negative” and “positive” groups (Figure 6A: 1st Gaussian: mean $\text{CL} = 0.6$, $\text{SD} = 13.2$ CL; 2nd Gaussian: mean = 84.4, $\text{SD} = 31.0$ CL), with expected differences by diagnostic stratum (Figure 6E). This behavior was observed for both tracers.

The frequency of CL values of 1545 baseline PNHS is shown in Figure 6B. The distribution for the PNHS is strongly skewed toward lower CL values and shows a relatively reduced range of CL values compared to that of the DPMS. This was expected given that the PNHS mainly recruited cognitively unimpaired participants (CDR = 0, as depicted in pink in Figure 6F). The PNHS showed a more skewed distribution toward higher Centiloids modeled with three Gaussians (based on the AIC): one for the negative group (mean = -0.4 , $\text{SD} = 6.3$ CL), one for the positive group (mean = 58.5, $\text{SD} = 36.6$ CL), and a third one in line with emerging pathology or lower bound of an “intermediate range”/gray-zone (mean = 8.9, $\text{SD} = 9.8$ CL).

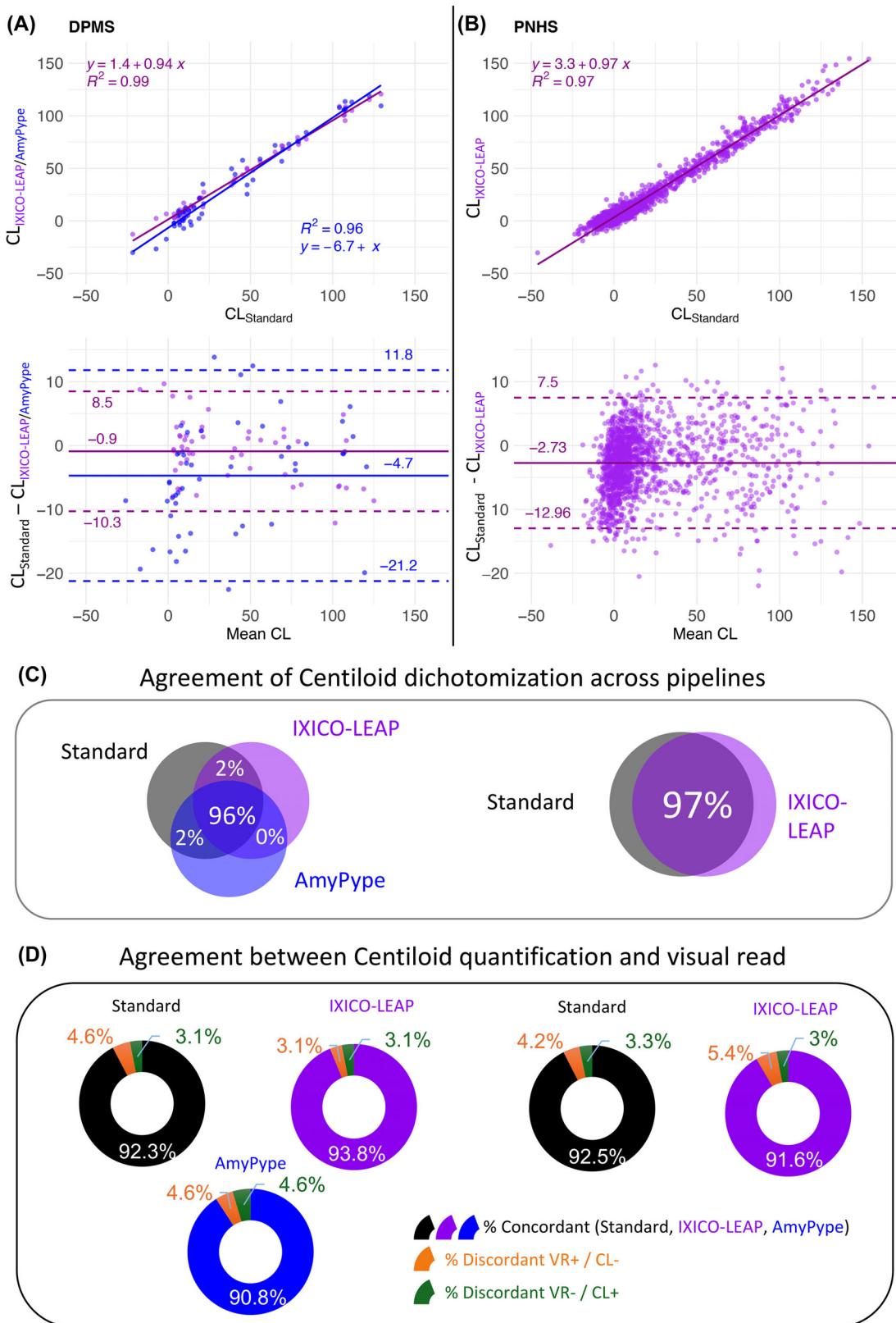
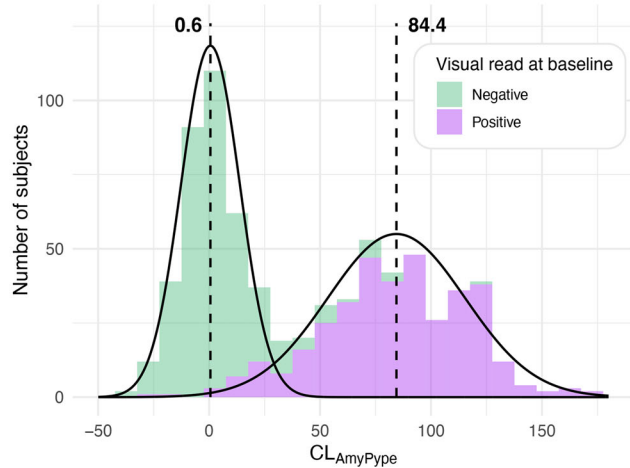
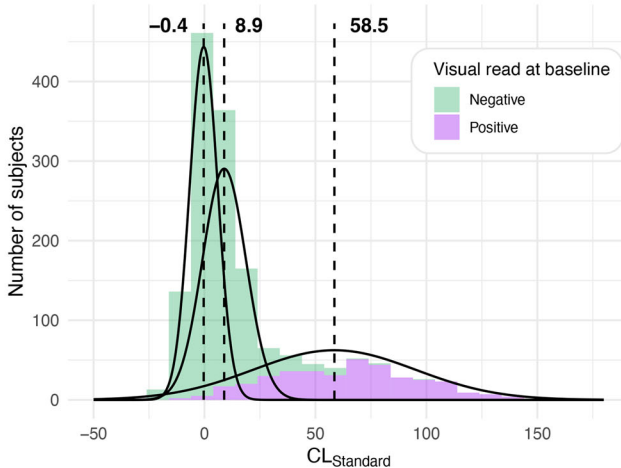


FIGURE 5 Comparison of three Centiloid pipeline: the standard Centiloid pipeline (in black), AmyPype (in blue), and IXICO-LEAP workflow (in purple). Correlation and Bland–Altman plots are shown for the DPMS (A) and the PNHS (B) datasets. Venn diagrams representing the percentage agreement between pipelines after dichotomization of Centiloid values are displayed in (C) (positivity defined as amyloid load > 24.4 CL, independent threshold based on histopathology^{13,37}). (D) Plots represent the percentage agreement between visual reads and quantification. CL, Centiloid; DPMS, Diagnostic and Patient Management Study; LEAP, learning embeddings for atlas propagation; PNHS, Prognostic and Natural History Study.

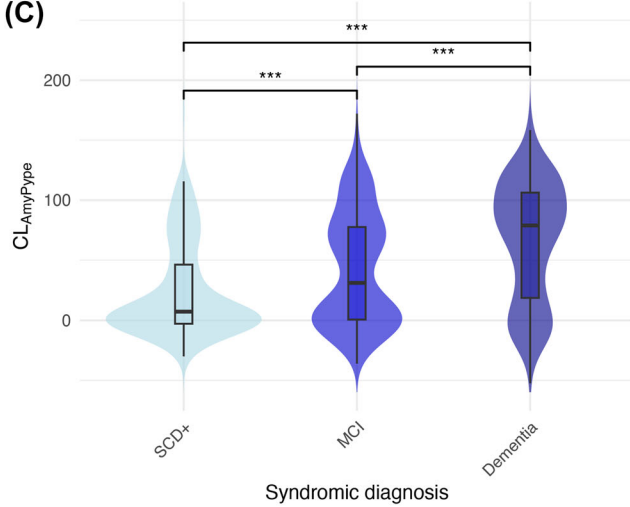
(A) DPMS



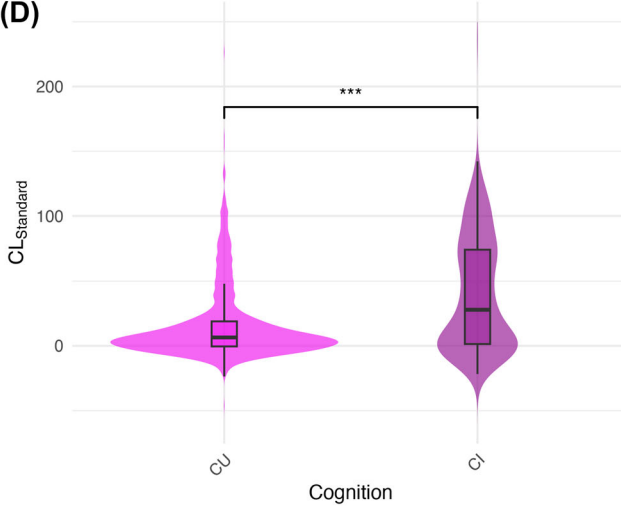
(B) PNHS



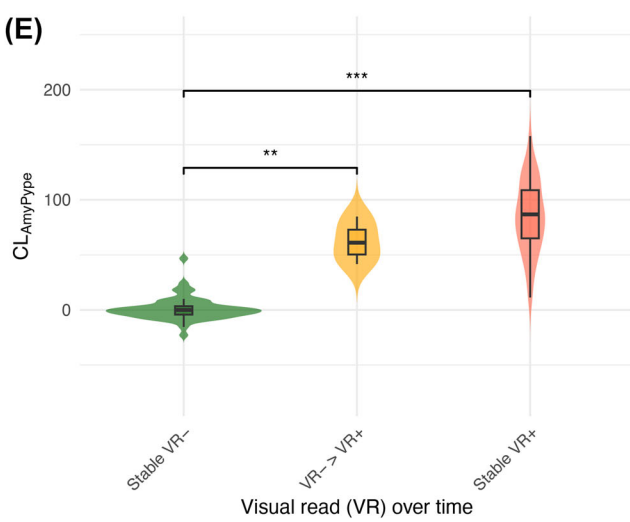
(C)



(D)



(E)



(F)

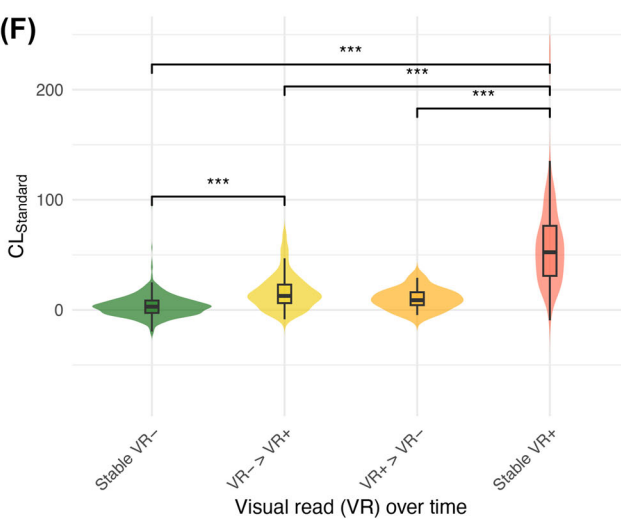


FIGURE 6 Distribution of Centiloid values in the DPMS and PNHS datasets. Centiloid values were presented here are from AmyPype for the DPMS and from the standard Centiloid pipeline for the PNHS. CU and CI in (D) correspond to CDR = 0 and CDR = 0.5, respectively. (E, F) Plots were obtained using the subsets of PNHS and DPMS with longitudinal data available ($N = 760$ and $N = 107$, respectively). CDR, Clinical Dementia Rating scale; CI, cognitively impaired individuals; CU, cognitively unimpaired individuals; DPMS, Diagnostic and Patient Management Study; MCI, mild cognitive impairment; PNHS, Prognostic and Natural History Study; SCD+, subjective cognitive decline +; VR, visual read.

4 | DISCUSSION

By implementing standardized acquisition protocols, phantom-based calibration with post-reconstruction harmonization strategies, we demonstrate that robust cross-center harmonization is feasible at scale. Importantly, our work highlight that different data processing approaches for Centiloid quantification can yield highly consistent results when harmonization and standardization principles are applied.

To assess the robustness of amyloid quantification, we conducted a comparative analysis of three Centiloid workflows: AmyPype, IXICO-LEAP workflow, and the standard Centiloid pipeline. We found a strong correlation among these methods, especially between the IXICO-LEAP and the standard Centiloid pipeline. In the DPMS subset, when comparing AmyPype to the other pipelines, we observed a small underestimation of low amyloid loads ($\lesssim 40$ CL) and overestimation of very high amyloid loads ($\gtrsim 100$ CL). However, the sample size was relatively small, and all pipelines showed very high agreement with visual reads (>90% concordance, Cohen's kappa ≥ 0.8 , or [0.67, 0.99] across all software). In the 10–60 CL subsample of the PNHS data covering the intermediate range (gray-zone), a higher proportion of discordant cases was found compared to the whole cohort, which is in line with results from the IDEAS real-world study.⁴⁰

While our work did not include a comparison with histopathology as the standard of truth, several studies have also evaluated currently available research and commercial tools providing a Centiloid output, including against histopathology, and showed generally consistent results across software.^{41–43} As anti-amyloid therapies are emerging, future studies comparing recently regulatory-approved software are warranted, to ensure that clinical decision-making is not influenced by the choice of amyloid quantification software.

Previous work from AMYPAD assessed the robustness of the Centiloid scale to many processing parameters, conducted by testing 32 combinations of pipeline settings.⁴⁴ In short, the CL was most influenced by the selection and delineation of reference regions. The whole cerebellum or “whole cerebellum + brainstem” provided consistent results across tracers while the pons and cerebellar gray matter are not recommended. Additionally, the standard Centiloid pipeline was shown to be robust against atrophy, differences in image resolution, and image harmonization. Importantly, while harmonization through smoothing based on accurate Hoffman-based measurements can reduce some of the variance between scanners, residual differences related to detector technology,⁴⁵ reconstruction methods, and noise properties remain and can affect Centiloid quantification.

From a clinical perspective, the distribution of Centiloid values reflects the expected patterns in clinical populations, with a bimodal distribution in the DPMS, indicative of distinct “negative” and “positive” amyloid groups, and a trimodal distribution in the PNHS, highlighting the successful recruitment of a sample enriched for individuals displaying incipient amyloid pathology. Interestingly in the PNHS, the mean + 2 SD of the ‘Normal’ Gaussian corresponds to 12.2 CL, which was the pathology-based threshold found to detect CERAD moderate-to-frequent neuritic plaques.³⁷ It is also in line with the lower cutoff of the “intermediate range” category established by the consortium.^{46,47}

The AMYPAD consortium experience offers several practical considerations for generalizability to other multi-center cohorts. First, harmonization requires early integration of standardized protocols across sites, supported by rigorous quality control. Second, harmonization of the effective image resolution by applying scanner-specific smoothing kernel can help mitigate heterogenous image quality across sites. Third, for amyloid-PET quantification, cross-validation between pipelines remains essential. It is recommended that studies adhere to the data acquisition guidelines provided for each tracer and follow the AMYPAD harmonization protocol, available on the EARL website, to prospectively harmonize their amyloid PET scans using pre-defined effective image resolutions. These considerations can support interoperability and comparability of amyloid-PET data across diverse research and clinical settings.

Clinical implications are equally important. While concordance between quantification approaches was high, residual differences between pipelines may influence amyloid positivity classification, which in turn could affect diagnostic and treatment decisions for AD at the individual level. Discordance between methods (whether across quantification pipelines or compared to visual reads), even if limited, carries the potential for misclassification, particularly near relevant or common threshold values. This highlights the need for caution when transitioning between pipelines, as well as the importance of validating thresholds within harmonized frameworks.

5 | CONCLUSION

The AMYPAD consortium has developed a comprehensive approach to amyloid-PET implementation. The distribution of Centiloid values in the PNHS and DPMS are in line with the initial recruitment strategies of the trials, which are well positioned to address pivotal research questions regarding early therapeutic interventions and the impact of lifestyle risk factors on AD progression. Additionally, the cross-validation of the Centiloid across software engenders confidence for the future use of amyloid PET for initiating and monitoring recently approved anti-amyloid therapies.

ACKNOWLEDGMENTS

The authors thank Bart van Berckel, Ronald Boelaard, and Adriaan Lammertsma for their contributions to the AMYPAD consortium. Data used in the preparation of this article were obtained from the Prognostic and Natural History Study (PNHS) and the Diagnostic and Patient Management Study (DPMS), provided by the amyloid imaging to prevent Alzheimer's Disease Consortium (AMYPAD). As such, investigators within the AMYPAD PNHS, AMYPAD DPMS, and AMYPAD Consortium contributed to the design and implementation of AMYPAD and/or provided data but did not participate in the analysis or writing of this report. A complete list of AMYPAD investigators can be found at <https://doi.org/10.5281/zenodo.7962737>. The project leading to this paper has received funding from the Innovative Medicines Initiative 2 Joint Undertaking under grant agreement No 115952. This Joint Undertaking receives the support from the European Union's Horizon

2020 research and innovation programme and EFPIA. This communication reflects the views of the authors and neither IMI nor the European Union and EFPIA are liable for any use that may be made of the information contained herein. The AMYPAD PNHS is registered at www.clinicaltrialsregister.eu with the EudraCT Number: 2018-002277-22. This work was supported by the Alzheimer's Disease Data Initiative (ADDI).

CONFLICT OF INTEREST STATEMENT

Ariane Bollack, Christopher Buckley, Anja Mett, and Gill Farrar are full-time employees of GE HealthCare. Alexander Drzezga has received research support from: Siemens Healthineers, Life Molecular Imaging, GE Healthcare, AVID Radiopharmaceuticals, Sofie, Eisai, Novartis/AAA, Ariceum Therapeutics, Speaker Honorary/Advisory Boards from: Siemens Healthineers, Sanofi, GE Healthcare, Biogen, Novo Nordisk, Invicro, Novartis/AAA, Bayer Vital, Lilly, Peer View Institute for Medical Education, International Atomic Energy Agency and owns stock from: Siemens Healthineers, Lilly. Frederik Barkhof is a Steering committee or Data Safety Monitoring Board member for Biogen, Merck, Eisai, and Prothena. Advisory board member for Combinostics, Scottish Brain Sciences, Alzheimer Europe. Consultant for Roche, Celltrion, Rewind Therapeutics, Merck, Bracco. Research agreements with ADDI, Merck, Biogen, GE Healthcare, Roche. Co-founder and shareholder of Queen Square Analytics LTD. Rossella Gismondi and Andrew Stephens are full-time employees of Life Molecular Imaging GmbH. Juan Domingo Gispert is a full-time employee of AstraZeneca. He has received research support from GE Healthcare, Roche Diagnostics, and Hoffmann-La Roche; has received speaker/consulting fees from Roche Diagnostics, Philips Nederlands, Esteve, Biogen, and Life Molecular Imaging; served in the Molecular Neuroimaging Advisory Board of Prothena Biosciences; and is funder and co-owner of BetaScreen SL. Robin Wolz is a full-time employee of IXICO. The other authors declare no competing interests. Author disclosures are available in the [Supporting Information](#).

CONSENT STATEMENT

All human participants provided informed consent.

ORCID

Ariane Bollack  <https://orcid.org/0000-0002-9169-7530>
 Mahnaz Shekari  <https://orcid.org/0000-0003-1336-6768>
 Lyduine E. Collij  <https://orcid.org/0000-0001-6263-1762>
 Emma Luckett  <https://orcid.org/0000-0003-1777-4742>
 David Valléz García  <https://orcid.org/0000-0003-3308-3167>
 Paweł Markiewicz  <https://orcid.org/0000-0002-3114-0773>
 Maqsood Yaqub  <https://orcid.org/0000-0002-8197-0118>
 Pieter Jelle Visser  <https://orcid.org/0000-0001-8008-9727>
 Alexander Drzezga  <https://orcid.org/0000-0001-6018-716X>
 Christopher Buckley  <https://orcid.org/0009-0005-3118-365X>
 Juan Domingo Gispert  <https://orcid.org/0000-0002-6155-0642>
 Gill Farrar  <https://orcid.org/0000-0002-0726-723X>
 Frederik Barkhof  <https://orcid.org/0000-0003-3543-3706>

REFERENCES

1. Scheltens P, De Strooper B, Kivipelto M, et al. Alzheimer's disease. *Lancet Lond Engl* 2021;397:1577-90. doi: [10.1016/S0140-6736\(20\)32205-4](https://doi.org/10.1016/S0140-6736(20)32205-4)
2. Clark CM, Schneider JA, Bedell BJ, et al. Use of florbetapir-PET for imaging β -amyloid pathology. *JAMA* 2011;305:275-83. doi: [10.1001/jama.2010.2008](https://doi.org/10.1001/jama.2010.2008)
3. Curtis C, Gamez JE, Singh U, et al. Phase 3 trial of flutemetamol labeled with radioactive fluorine 18 imaging and neuritic plaque density. *JAMA Neurol* 2015;72:287-94. doi: [10.1001/jamaneurol.2014.4144](https://doi.org/10.1001/jamaneurol.2014.4144)
4. Barthel H, Gertz H-J, Dresel S, et al. Cerebral amyloid- β PET with florbetaben (18F) in patients with Alzheimer's disease and healthy controls: a multicentre phase 2 diagnostic study. *Lancet Neurol* 2011;10:424-35. doi: [10.1016/S1474-4422\(11\)70077-1](https://doi.org/10.1016/S1474-4422(11)70077-1)
5. Chapleau M, Iaccarino L, Soleimani-Meigooni D, Rabinovici GD. The role of amyloid PET in imaging neurodegenerative disorders: A review. *J Nucl Med* 2022;63:13S-19S. doi: [10.2967/jnmed.121.263195](https://doi.org/10.2967/jnmed.121.263195)
6. Sims JR, Zimmer JA, Evans CD, et al. Donanemab in early symptomatic Alzheimer disease: The trailblazer-ALZ 2 randomized clinical trial. *JAMA* 2023;330(6):512-527. doi: [10.1001/jama.2023.13239](https://doi.org/10.1001/jama.2023.13239)
7. van Dyck CH, Swanson CJ, Aisen P, et al. Lecanemab in early Alzheimer's disease. *N Engl J Med* 2023;388:9-21. doi: [10.1056/NEJMoa2212948](https://doi.org/10.1056/NEJMoa2212948)
8. Collij LE, Konijnenberg E, Reimand J, et al. Assessing amyloid pathology in cognitively normal subjects using 18F-Flutemetamol PET: Comparing visual reads and quantitative methods. *J Nucl Med* 2019;60:541-7. doi: [10.2967/jnmed.118.211532](https://doi.org/10.2967/jnmed.118.211532)
9. Collij LE, Heeman F, Salvadó G, et al. Multitracer model for staging cortical amyloid deposition using PET imaging. *Neurology* 2020;95:e1538-53. doi: [10.1212/WNL.0000000000010256](https://doi.org/10.1212/WNL.0000000000010256)
10. Palmqvist S, Tideman P, Cullen N, et al. Prediction of future Alzheimer's disease dementia using plasma phospho-tau combined with other accessible measures. *Nat Med* 2021;27:1034-42. doi: [10.1038/s41591-021-01348-z](https://doi.org/10.1038/s41591-021-01348-z)
11. Pemberton HG, Collij LE, Heeman F, et al. Quantification of amyloid PET for future clinical use: A state-of-the-art review. *Eur J Nucl Med Mol Imaging* 2022;49:3508-28. doi: [10.1007/s00259-022-05784-y](https://doi.org/10.1007/s00259-022-05784-y)
12. Klunk WE, Koeppe RA, Price JC, et al. The Centiloid project: Standardizing quantitative amyloid plaque estimation by PET. *Alzheimers Dement J Alzheimers Assoc* 2015;11:1-15. e4. doi: [10.1016/j.jalz.2014.07.003](https://doi.org/10.1016/j.jalz.2014.07.003)
13. Collij LE, Bollack A, La Joie R, et al. Centiloid recommendations for clinical context-of-use from the AMYPAD consortium. *Alzheimers Dement* 2024;20(12):9037-9048. doi: [10.1002/alz.14336](https://doi.org/10.1002/alz.14336)
14. Frisoni GB, Barkhof F, Altomare D, et al. AMYPAD diagnostic and patient management study: Rationale and design. *Alzheimers Dement* 2019;15:388-99. doi: [10.1016/j.jalz.2018.09.003](https://doi.org/10.1016/j.jalz.2018.09.003)
15. Lopes Alves I, Collij LE, Altomare D, et al. Quantitative amyloid PET in Alzheimer's disease: The AMYPAD prognostic and natural history study. *Alzheimers Dement* 2020;16:750-8. doi: [10.1002/alz.12069](https://doi.org/10.1002/alz.12069)
16. Altomare D, Collij L, Caprioglio C, et al. Description of a European memory clinic cohort undergoing amyloid-PET: The AMYPAD Diagnostic and Patient Management Study. *Alzheimers Dement* 2023;19:844-56. doi: [10.1002/alz.12696](https://doi.org/10.1002/alz.12696)
17. Ritchie CW, Molinuevo JL, Trynen L, Satlin A, der Geyten SV, Lovestone S. Development of interventions for the secondary prevention of Alzheimer's dementia: The European prevention of Alzheimer's dementia (EPAD) project. *Lancet Psychiatry* 2016;3:179-86. doi: [10.1016/S2215-0366\(15\)00454-X](https://doi.org/10.1016/S2215-0366(15)00454-X)
18. Konijnenberg E, Carter SF, ten Kate M, et al. The EMIF-AD PreclinAD study: Study design and baseline cohort overview. *Alzheimers Res Ther* 2018;10:75. doi: [10.1186/s13195-018-0406-7](https://doi.org/10.1186/s13195-018-0406-7)
19. Molinuevo JL, Gramunt N, Gispert JD, et al. The ALFA project: A research platform to identify early pathophysiological features

of Alzheimer's disease. *Alzheimers Dement Transl Res Clin Interv* 2016;2:82-92. doi: [10.1016/j.trci.2016.02.003](https://doi.org/10.1016/j.trci.2016.02.003)

20. Rodriguez-Gomez O, Sanabria A, Perez-Cordon A, et al. FACEHBI: A prospective study of risk factors, biomarkers and cognition in a cohort of individuals with subjective cognitive decline. study rationale and research protocols. *J Prev Alzheimers Dis* 2017;4:100-8. doi: [10.14283/jpad.2016.122](https://doi.org/10.14283/jpad.2016.122)

21. Schaeverbeke JM, Gabel S, Meersmans K, et al. Baseline cognition is the best predictor of 4-year cognitive change in cognitively intact older adults. *Alzheimers Res Ther* 2021;13:75. doi: [10.1186/s13195-021-00798-4](https://doi.org/10.1186/s13195-021-00798-4)

22. Jessen F, Spottke A, Boecker H, et al. Design and first baseline data of the DZNE multicenter observational study on predementia Alzheimer's disease (DELCODE). *Alzheimers Res Ther* 2018;10:15. doi: [10.1186/s13195-017-0314-2](https://doi.org/10.1186/s13195-017-0314-2)

23. Rydberg Sterner T, Ahlner F, Blennow K, et al. The Gothenburg H70 Birth cohort study 2014-16:Design, methods, and study population. *Eur J Epidemiol* 2019;34:191-209. doi: [10.1007/s10654-018-0459-8](https://doi.org/10.1007/s10654-018-0459-8)

24. Bader I, Bader I, Lopes Alves I, et al. Recruitment of pre-dementia participants: Main enrollment barriers in a longitudinal amyloid-PET study. *Alzheimers Res Ther* 2023;15:189. doi: [10.1186/s13195-023-01332-4](https://doi.org/10.1186/s13195-023-01332-4)

25. Heeman F, Yaqub M, Lopes Alves I, et al. Optimized dual-time-window protocols for quantitative [18F]flutemetamol and [18F]florbetaben PET studies. *EJNMMI Res* 2019;9:32. doi: [10.1186/s13550-019-0499-4](https://doi.org/10.1186/s13550-019-0499-4)

26. Aide N, Lasnon C, Veit-Haibach P, Sera T, Sattler B, Boellaard R. EANM/EARL harmonization strategies in PET quantification: From daily practice to multicentre oncological studies. *Eur J Nucl Med Mol Imaging* 2017;44:17-31. doi: [10.1007/s00259-017-3740-2](https://doi.org/10.1007/s00259-017-3740-2)

27. Buckley C, Foley C, Battle M, et al. AmyPype: An automated system to quantify AMYPAD's [18 F]flutemetamol and [18 F]florbetaben images including regional SUVR and Centiloid analysis, EANM 2019;19.

28. Life Radiopharma Berlin GmbH. Neuraceq : EPAR—Product Information. EMEA/H/C/002553. Eur Med Agency 2022. <https://www.ema.europa.eu/en/medicines/human/EPAR/neuraceq>

29. GE HealthCare. Vizamyl : EPAR—Product Information. EMEA/H/C/002557. Eur Med Agency 2023. <https://www.ema.europa.eu/en/medicines/human/EPAR/vizamyl>

30. Shekari M, Verwer EE, Yaqub M, et al. Harmonization of brain PET images in multi-center PET studies using Hoffman phantom scan. *EJNMMI Phys* 2023;10:68. doi: [10.1186/s40658-023-00588-x](https://doi.org/10.1186/s40658-023-00588-x)

31. Collij LE, Bischof GN, Altomare D, et al. Quantification supports visual assessment of challenging amyloid-PET images. *Alzheimers Dement* 2023;19:e074620. doi: [10.1002/alz.074620](https://doi.org/10.1002/alz.074620)

32. Lundqvist R, Lilja J, Thomas BA, et al. Implementation and validation of an adaptive template registration method for 18F-Flutemetamol imaging data. *J Nucl Med* 2013;54:1472-8. doi: [10.2967/jnumed.112.115006](https://doi.org/10.2967/jnumed.112.115006)

33. Rolls ET, Huang C-C, Lin C-P, Feng J, Joliot M. Automated anatomical labelling atlas 3. *NeuroImage* 2020;206:116189. doi: [10.1016/j.neuroimage.2019.116189](https://doi.org/10.1016/j.neuroimage.2019.116189)

34. Wolz R, Aljabar P, Hajnal JV, Hammers A, Rueckert D. LEAP: Learning embeddings for atlas propagation. *NeuroImage* 2010;49:1316-25. doi: [10.1016/j.neuroimage.2009.09.069](https://doi.org/10.1016/j.neuroimage.2009.09.069)

35. Grecchi E, Wolz R, Hill DL. [p4-234]: Operationalizing automated pet suvr quantification in multi-centre ad clinical trials. *Alzheimers Dement* 2017;13:P1362-4. doi: [10.1016/j.jalz.2017.06.2102](https://doi.org/10.1016/j.jalz.2017.06.2102)

36. Desikan RS, Ségonne F, Fischl B, et al. An automated labeling system for subdividing the human cerebral cortex on MRI scans into gyral based regions of interest. *NeuroImage* 2006;31:968-80. doi: [10.1016/j.neuroimage.2006.01.021](https://doi.org/10.1016/j.neuroimage.2006.01.021)

37. La Joie R, Ayakta N, Seeley WW, et al. Multisite study of the relationships between *antemortem* [¹¹ C]PIB-PET Centiloid values and *post-mortem* measures of Alzheimer's disease neuropathology. *Alzheimers Dement* 2019;15:205-16. doi: [10.1016/j.jalz.2018.09.001](https://doi.org/10.1016/j.jalz.2018.09.001)

38. Alzheimer's Disease Data Initiative WorkBench n.d. <https://www.alzheimersdata.org/>

39. Health RI XNAT platform—AMYPAD n.d. <https://xnat.health-ri.nl/data/projects/amypad>

40. Zeltzer E, Schonhaut DR, Mundada NS, et al. Concordance between amyloid-PET quantification and real-world visual reads: results from IDEAS. 2024:2024.10.31.24316518. doi: [10.1101/2024.10.31.24316518](https://doi.org/10.1101/2024.10.31.24316518)

41. Jovalekic A, Roé-Vellvé N, Koglin N, et al. Validation of quantitative assessment of florbetaben PET scans as an adjunct to the visual assessment across 15 software methods. *Eur J Nucl Med Mol Imaging* 2023;50(11):3276-3289. doi: [10.1007/s00259-023-06279-0](https://doi.org/10.1007/s00259-023-06279-0)

42. Shang C, Sakurai K, Nihashi T, et al. Comparison of consistency in centiloid scale among different analytical methods in amyloid PET: The CapAIBL, VIZCalc, and Amyquant methods. *Ann Nucl Med* 2024;38:460-7. doi: [10.1007/s12149-024-01919-3](https://doi.org/10.1007/s12149-024-01919-3)

43. Doré V, Bullich S, Rowe CC, et al. Comparison of 18F-florbetaben quantification results using the standard Centiloid, MR-based, and MR-less CapAIBL® approaches: Validation against histopathology. *Alzheimers Dement* 2019;15:807-16. doi: [10.1016/j.jalz.2019.02.005](https://doi.org/10.1016/j.jalz.2019.02.005)

44. Shekari M, Vállez García D, Collij LE, et al. Stress testing the Centiloid: Precision and variability of PET quantification of amyloid pathology. *Alzheimers Dement* 2024;20:5102-13. doi: [10.1002/alz.13883](https://doi.org/10.1002/alz.13883)

45. Gillman A, Bourgeat P, Cox T, et al. Digital detector PET/CT increases Centiloid measures of amyloid in Alzheimer's disease: A head-to-head comparison of cameras. *J Alzheimer's Dis* 2025;103:1257-68. doi: [10.1177/13872877241313063](https://doi.org/10.1177/13872877241313063)

46. Collij LE, Bollack A, La Joie R, et al. Centiloid recommendations for clinical context-of-use from the AMYPAD consortium. *Alzheimers Dement* 2024;20:9037-48. doi: [10.1002/alz.14336](https://doi.org/10.1002/alz.14336)

47. Salvadó G, Molinuevo JL, Brugulat-Serrat A, et al. Centiloid cut-off values for optimal agreement between PET and CSF core AD biomarkers. *Alzheimers Res Ther* 2019;11:27. doi: [10.1186/s13195-019-0478-z](https://doi.org/10.1186/s13195-019-0478-z)

SUPPORTING INFORMATION

Additional supporting information can be found online in the Supporting Information section at the end of this article.

How to cite this article: Bollack A, Shekari M, Collij LE, et al. Implementing robust amyloid PET quantification in multi-center studies: AMYPAD approach to address data acquisition, processing, interpretation and data sharing challenges. *Alzheimer's Dement.* 2025;11:e70190.

<https://doi.org/10.1002/trc2.70190>